Carbon nanotube growth on Ni-particles prepared in situ by reduction of La$_2$NiO$_4$

Q. Liang, L.Z. Gao, Q. Li, S.H. Tang, B.C. Liu, Z.L. Yu[*]

Chengdu Institute of Organic Chemistry, Chinese Academy of Sciences, Chengdu 610041, PR China

Abstract

Using the citric acid complexing method, perovskite-like mixed oxides La$_2$NiO$_4$ were prepared. Before and after reduction, its structure was characterized by means of X-ray diffraction and XPS. Due to the formation of La$_2$NiO$_4$, Ni^{2+} and La^{3+} ions were evenly distributed. Nickel exists chiefly as Ni^0 after reduction and the size of Ni particles was estimated to be ca. 28 nm. After reduction of La$_2$NiO$_4$ oxide, the rare earth oxide, La$_2$O$_3$, prevents Ni particles from agglomerating and promotes the dispersion of nano-scale Ni particles, which is one of the key factors for carbon nanotube growth. The carbon nanotubes from the catalytic decomposition of CH$_4$ were obtained using La$_2$NiO$_4$ oxides as the catalyst precursor. The morphology of the carbon nanotubes obtained has been examined by transmission electron microscopy and scanning electron microscopy. High resolution transmission electron microscopy images and Raman spectra of carbon nanotubes show they are multi-walled nanotubes of good quality. © 2001 Elsevier Science Ltd. All rights reserved.

Keywords: A. Carbon nanotubes; B. Catalyst; C. Transmission electron microscopy; D. Crystallite size

1. Introduction

Carbon nanotubes (CNTs), as a new allotrope of carbon with extraordinary properties and potential applications, have attracted much interest since they were discovered in 1991 by Iijima [1]. Now the synthesis of CNTs is one of the challenging issues in the new carbon materials field. Several techniques have been developed for CNT growth such as arc discharge [2], laser vaporization [3], and catalytic thermal decomposition of hydrocarbons [4]. The catalytic production of CNTs is simpler and more reproducible than other methods. Recently, decomposition of hydrocarbons has become a research focus for the growth of CNTs and they have been obtained by the decomposition of CH$_4$ [5], C$_2$H$_2$ [6], CO [7], benzene [8], polyethene [9] etc. There is an abundant supply of CH$_4$ in the world and relatively few means of converting it to more valuable products. The conversion of CH$_4$ has attracted more

attention all over the world. Synthesis of CNTs on a large scale by the catalytic technique is an attractive and hopefully alternative route. Though there are many factors involved such as temperature, pressure, feedstock gas, reaction time, and flow rate, the size of transition metal particles is found to be influential for the formation of CNTs [10]. With this method, therefore, it is crucial to select an effective catalyst with the appropriate size of active metal. Several mechanisms have been proposed to attempt at explanation of CNT formation and growth by the pyrolysis of hydrocarbons over catalysts [11,12].

Mixed metal oxides with perovskite-type and perovskite-like structure have recently been investigated extensively as the catalyst for many chemical reactions, for example, hydrocarbon combustion and NH$_3$ oxidation [13]. They are all well defined oxide solid solutions. The oxidation states of transition metals can be changed by modifying the constituent elements and the preparation conditions. The size of the active transition metal particles may be controlled to some extent by changing the reduction conditions. In the present work, we firstly used perovskite-like metal oxides as catalyst precursors for CNTs growth. The bulk growth of CNTs was obtained by

*Corresponding author. Tel.: +86-28-5229-790; fax: +86-28-5229-790.

E-mail address: yzuolong@mail.sc.cninfo.net (Z.L. Yu).

the catalytic decomposition of CH_4 over Ni nano-particles from pre-reduced La_2NiO_4 oxide. With this kind of catalyst, some important advantages of preparing nanotubes are obvious. The product yield is higher and the reaction temperature is lower compared with the other method. The diameter of the CNTs is uniform and their purification and separation is easy due to the support-free catalyst.

2. Experimental

The La_2NiO_4 oxide was prepared by adopting the citric acid complexing method, namely, decomposition of amorphous precursors (citrates) [13]. Briefly, to a mixed aqueous solution of $Ni(NO_3)_2 \cdot 6H_2O$ and $La(NO_3)_3 \cdot 6H_2O$ with appropriate stoichiometry, 100% excess of citric solution was added. All compounds used were AR grade. The resulting gel was evaporated at 353 K with stirring until a viscous syrup was formed. The obtained residue was calcined in air at 773 K for 4 h and then pelleted prior to calcination at 1073 K for 6 h. The pulverized samples (ca. 60–80 mesh) were used as the catalyst precursor for the preparation of CNTs.

A horizontal quartz glass reactor, 30 mm in diameter and 1000 mm in length, was used for the growth of the CNTs. The heat source was a tubular electric furnace. The isothermal zone was 400 mm long in the middle of the tube. Temperatures were monitored using thermocouples coated with thin quartz tubes inserted into the quartz reactor. The gas flow into the reactor was controlled by mass flow controllers with an accuracy of ±0.1 ml for all gases. In all experiments, the reaction pressure was maintained at ambient.

The catalyst precursor was placed in a quartz boat (200 mm in length) and inserted into the reactor. The amount of catalyst in the oxidized state used for all experiments was 100 mg. First, the samples were reduced in a flow of H_2 (20 ml/min) from room temperature to 1073 K and and held there for 0.5 h. Then the reactor temperature was lowered to 973 K for the in situ reaction. After sweeping with Ar gas, CH_4 was introduced into the reactor, passing over the catalyst at 30 ml/min for 60 min. After cooling to ambient temperature in a flow of Ar, the products were collected and purified by washing with a solution of acid in order to remove the metal particles. The carbon residue was washed using de-ionized water until the pH value of the effluent solution was close to 7 and dried at 573 K in a flow of Ar.

The product sample was sonicated in acetone and dispersed onto a copper grid for microscopic examination. The morphologies and microstructure of the obtained CNTs have been examined using a scanning electron microscope (JEOL JXA-840), and low (JEOL JEM-100CX) and high-resolution (Hitachi 8100 and Philips
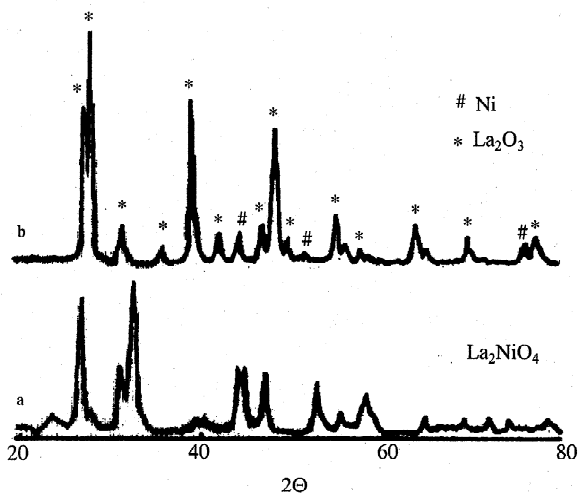

Fig. 1. X-ray diffraction patterns of the catalyst sample (a) before reduction (b) after reduction.

CM200 FEG, operated at 200 keV) transmission electron microscopes. The CNTs were also characterized by using a Rigaku Rotaflex D/Max-C X-ray diffractometer (XRD) with CuK radiation at a scanning rate of 2°/min from 10° to 90°. An Ar^+ ion laser beam of wavelength 514.5 nm was used to measure the spectra of the CNTs. The catalyst was also analyzed by SEM and energy dispersive X-ray microanalysis. A D/Max-C X-ray diffractometer was employed to measure the XRD profiles of the catalyst precursor and the Ni particle size was estimated from the peak half width. For the XPS analysis the reference binding energy was that of C (1s), 284.6 eV.

3. Results and discussion

3.1. The XRD and XPS study of the catalyst

Fig. 1a shows the X-ray diffraction pattern of the perovskite-like oxide, La_2NiO_4, which is identified as single phase with a tetragonal K_2NiF_4 structure. This result also revealed that the oxide with a A_2BO_4 structure

Table 1
XPS data of La_2NiO_4

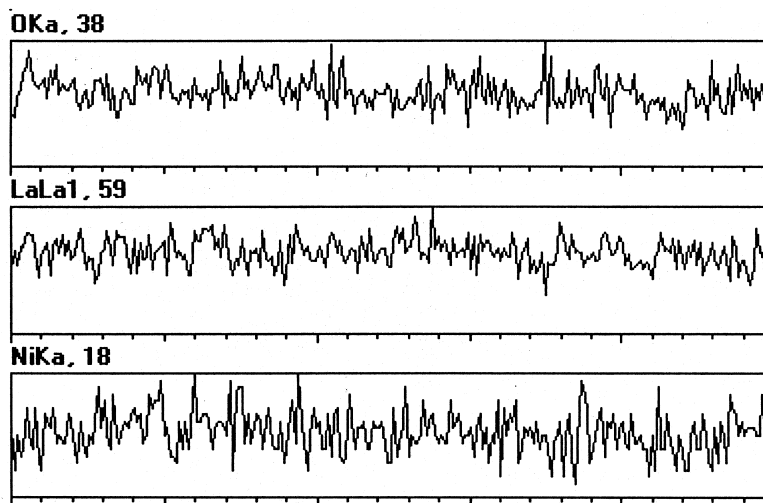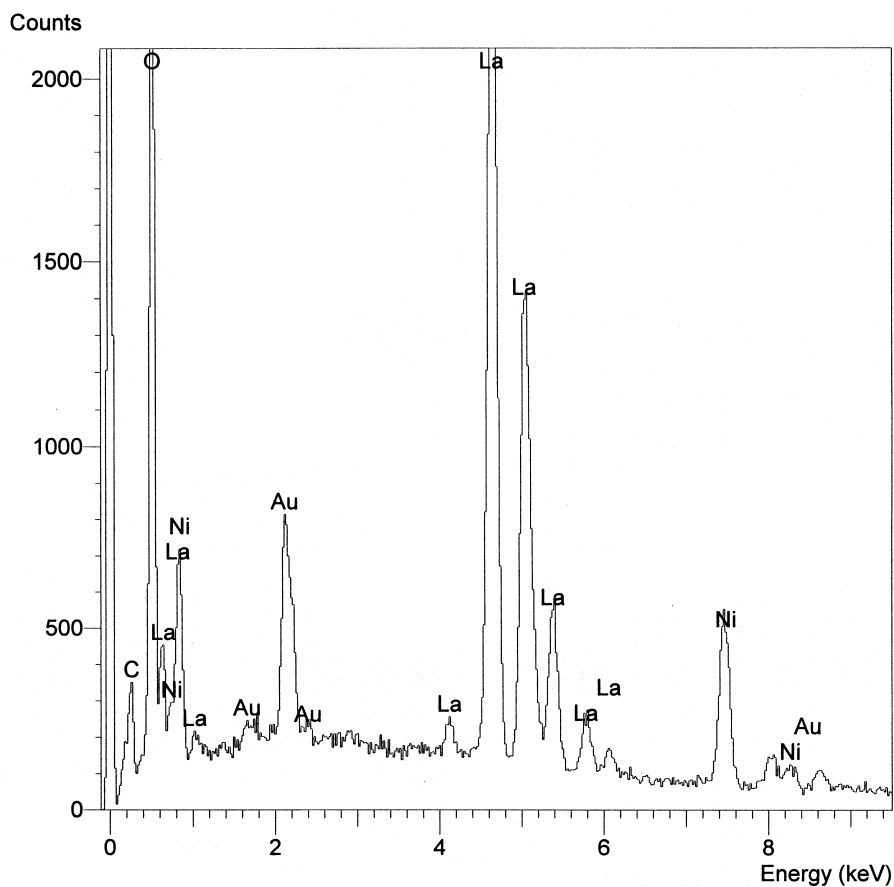| Before or after reduction	Ni $2p_{3/2}$ (eV)	La $3d_{5/2}$ (eV)
before	854.3	835.1
after	852.3	834.9

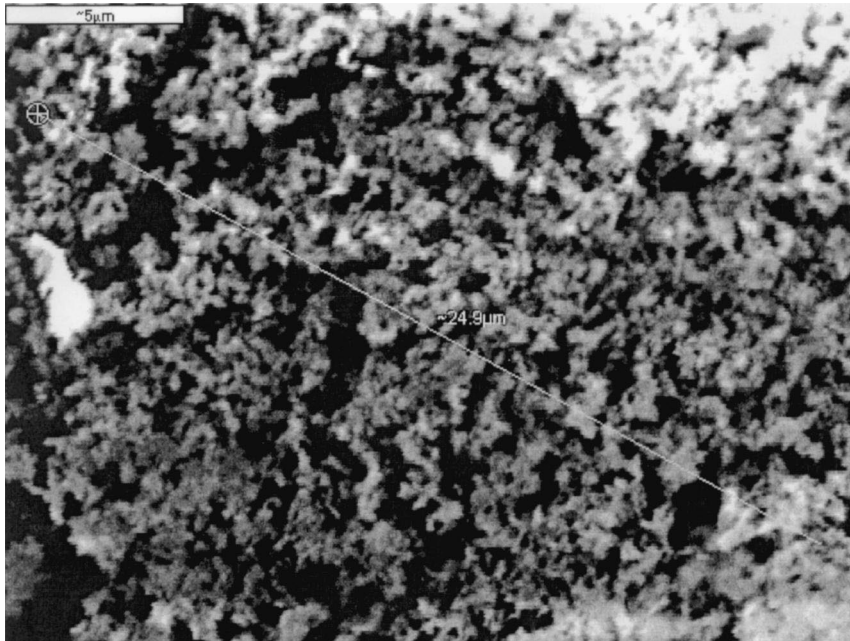Fig. 2. EDX spectrum and SEM image of reduced catalyst at 1073 K.

Fig. 2. (*continued*)

is stable due to the formation of La_2NiO_4, Ni^{2+} and La^{3+} ions were evenly distributed. The pattern for La_2NiO_4 reduced at 1073 K in H_2 is shown in Fig. 1b. This indicates that nickel exists chiefly as Ni^0 after reduction. The diameter of the Ni^0 particles was estimated to be ca. 28 nm. We suggest that the rare earth oxide, La_2O_3, can prevent transition metal from agglomerating and promotes the dispersion of nano-scale Ni particles, which is very advantageous for CNT growth [10].

XPS results of La_2NiO_4 before and after reduction are summarized in Table 1. It can be seen that before reduction the binding energy of Ni $2p_{3/2}$ is 854.3 eV, which is approximately that of NiO, indicating that nickel exists as Ni^{2+} in La_2NiO_4. However, after reduction the binding energy of Ni $2p_{3/2}$ is 852.3 eV, which tells us that Ni^{2+} turns mainly into Ni^0. Unlike Ni $2p_{3/2}$, the binding energy of La $3d_{5/2}$ does not change within experimental error. It can be concluded that lanthanum still exists as La^{3+}, but the mixed oxide La_2NiO_4 has been destroyed and the remnant is Ni/La_2O_3. Thus the active site Ni^0 particles are
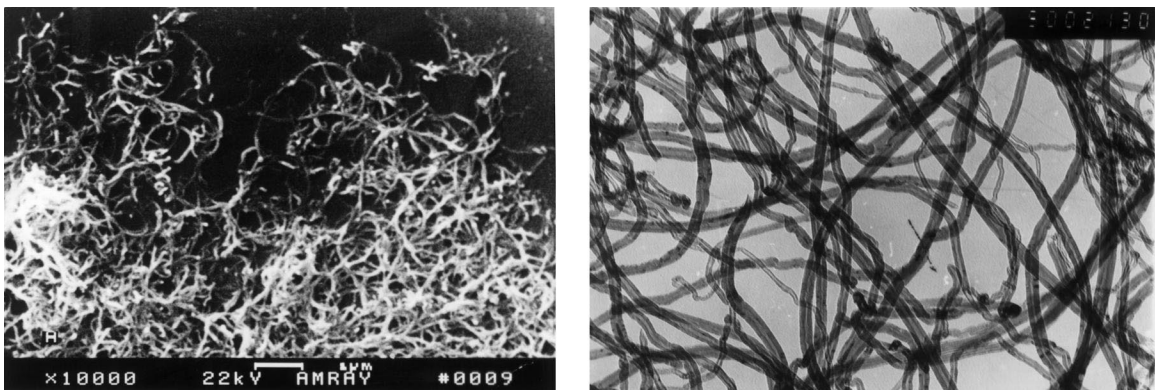
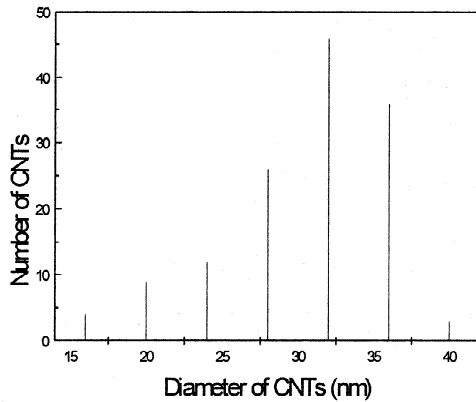Fig. 3. SEM and TEM image of CNTs prepared by decomposition of CH_4.

Fig. 4. Diameter distribution of CNTs.

supported and isolated by rare earth oxides. La_2O_3 plays a crucial role as the partition to restrict the size of Ni^0 particles.

3.2. SEM and EDX analysis of the catalyst

Fig. 2 shows a SEM image and the EDX spectrum of the catalyst after reduction. Well-dispersed catalyst can be observed in the SEM. According to EDX, the approximate La/Ni atom ratio was 2:1 and the three elements (O, La, Ni) were uniformly distributed. Thus we propose that this technique is a good and convenient method to disperse the active metal.
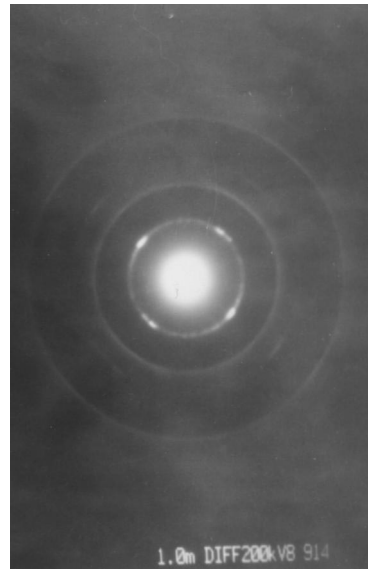

Fig. 5. SAED pattern of CNTs.

3.3. SEM and TEM study of CNTs

The CNTs were prepared by the decomposition of CH_4 at 973 K over the catalyst pre-reduced at 1073 K. Fig. 3a is a characteristic SEM image of CNTs with crooked and entangled shapes, which are similar to those in the literature [14]. We can see that the length of most CNTs is
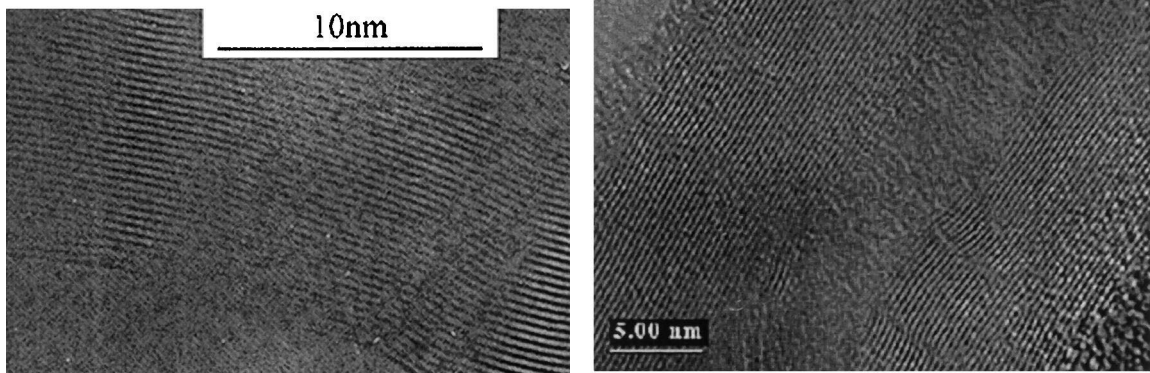

Fig. 6. HRTEM image of CNTs showing the multi-walled nanotubes composed of well graphitized layers usually covered with amorphous carbon on the outer periphery.

of the order of micron. After reaction 1 h, 512 mg CNTs can be synthesized with 100 mg catalyst (per furnace). The purity of CNTs was approximate to 96 percent. A typical TEM image (Fig. 3b) shows many rope-like structures of with outer diameters ranging from 15 to 40 nm. Fig. 4 shows the measured diameter distribution. Most of them are 25–35 nm, which is close to the size of the Ni particles. Most of the Ni particles capped on the nanotube tip or were encapsulated by carbonaceous tubes. The growth mechanism of CNTs on the transition metal is not completely clear yet. However, we found that the metal particles play a important role in the formation of CNTs. Compared with the CNTs from benzene [8], well graphitized CNTs were exhibited by SAED pattern (Fig. 5) and HRTEM (Fig. 6). Some helices were also found in the products. HRTEM images confirm the presence of multi-walled carbon nanotubes, which are composed of many cylindrical graphite layers arranging regularly in the inner wall. However we can also see that some amorphous carbon layers coat the outer periphery of carbon nanotubes.

3.4. XRD and Raman study of CNTs

X-ray diffraction was performed on the carbon products in order to study the microscopic structure of the CNTs. There was a strong and broad peak for turbostratic carbon at $26.4°$, giving an interlayer spacing (d_{002}) for the multi-walled CNTs, slightly larger than that of ideal graphite. In addition Ni crystallite peaks can be observed at ca. $44°$, $52°$ and $76°$ due to some Ni crystallite enwrapped by carbon. Fig. 7 shows the Raman shift spectrum of the CNTs, which was measured at room temperature with a frequency range $200–3500$ cm^{-1}. Two sharp peaks are present at 1570 (G peak) and 1326 (D peak) cm^{-1}. These correspond to the characteristic peak of the graphite structure with a small basal domain size [15]. Also near 2643 (2D or D* peak)
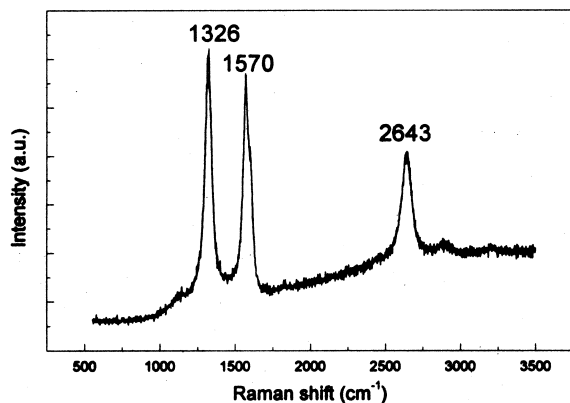
and 2920 (D+G peak) cm^{-1} there are two weaker peaks. Those features, including the wavenumbers and relative integrated intensities, are close to those for multi-walled carbon nanotubes [16], also those tell us that the grahitization degree of the outer wall is low, in agreement with the HRTEM results.

4. Conclusion

Bulk growth of CNTs from CH$_4$ was obtained using La$_2$NiO$_4$ oxide as the catalyst precursor. La$_2$O$_3$ prevents the transition metal from agglomerating and promotes the dispersion of nano-scale Ni particles after reduction, which is frequently responsible for CNT growth. The Raman spectrum and HRTEM features of the CNTs show that they are similar to well graphitized multi-walled carbon nanotubes.

Acknowledgements

References

[1] Iijima S. Helical microtubules of graphitic carbon. Nature 1991;354:56–8.
[2] Ebbesen TW, Ajayan M. Large-scale synthesis of carbon nanotubes. Nature 1992;358:220–2.
[3] Thess A, Lee R, Nikolaev P, Dai HJ, Petit P, Robert J et al. Crystalline ropes of metallic carbon nanotubes. Science 1996;273:483–7.
[4] Cheng HM, Li F, Sun X, Brown SDM, Pimenta MA, Marucci A et al. Bulk morphology and diameter distribution of single-walled carbon nanotubes synthesized by catalytic decomposition of hydrocarbons. Chem Phys Lett 1998;289:602–10.
[5] Ruckenstein E, Hu YH. Catalytic preparation of narrow pore size distribution mesoporous carbon. Carbon 1998;36:269–75.
[6] Li WZ, Xie SS, Qian LX, Chang BH, Zou BS, Zhou WY et al. Large-scale synthesis of aligned carbon nanotubes. Science 1996;274:1701–3.
[7] Chen P, Zhang HB, Lin GD, Hong Q, Ksai KR. Growth of carbon nanotubes by catalytic decomposition of CH$_4$ or CO on a Ni–MgO catalyst. Carbon 1997;35:1495–501.
[8] Benito AM, Maniette Y, Munoz E, Martinez MT. Carbon nanotubes production by catalytic pyrolysis of benzene. Carbon 1998;36:681–3.

Fig. 7. Raman spectrum of CNTs excited by 514.5 nm laser.

[9] Kukovitskii EF, Chernozatonskii LA, L'vov SG, Mel'nik NN. Carbon nanotubes of polyethylene. Chem Phys Lett 1998;289:602.

[10] Pan ZW, Xie SS, Chang BH, Sun LF, Zhou WY, Wang G. Direct growth of aligned open carbon nanotubes by chemical vapor deposition. Chem Phys Lett 1999;299:97–102.

[11] Amelinckx S, Zhang XB, Bernaerts D, Zhang XF, Ivanov V, Nagy JB. A formation mechanism for catalytically grown helix-shaped graphite nanotubes. Science 1994;265:635–9.

[12] Kong J, Cassel AM, Dai HJ. Chemical vapor deposition of methane for single-walled carbon nanotubes. Chem Phys Lett 1998;292:567–74.

[13] Yu ZL, Gao LZ, Yuan SY, Wu Y. Solid defect structure and catalytic activity of perovskite-type catalysts $La_{1-x}Sr_xNiO_{3-\lambda}$ and $La_{1-1.333x}Th_xNiO_{3-\lambda}$. J Chem Soc Faraday Trans 1992;88:3245–9.

[14] Muller TE, Reid DG, Hse WK, Hare JP, Kroto HW, Walton DRM. Synthesis of nanotubes via catalytic pyrolysis of acetylene: a SEM study. Carbon 1997;35:951–66.

[15] Yudasaka M, Komatse T, Ichihashi T, Achiba Y, Iijama S. Pressure dependence of structure of carbonaceous deposits formed by laser ablation on target composed of carbon, nickel, cobalt. J Phys Chem B 1998;102:4892–6.

[16] Tan PH, Zhang SL, Yue KT, Huang FM, Shi ZJ, Zhou XH et al. Comparative raman study of carbon nanotubes prepared by D.C. arc discharge and catalytic methods. J Raman Spectrosc 1997;28:369–72.